Electronic Supplementary Material (ESI) for Journal of Materials Chemistry A.

Supporting Information

Construction of Polyimide Structures Containing Iron(II) Clathrochelate Intercalators: Promising Materials for CO_2 Gas Uptake and Salient Adsorbents of Iodine from the Gaseous and Liquid Phases

Suchetha Shetty,[1,2] Noorullah Baig,[1,2] Mikhael Bechelany,[3] and Bassam Alameddine*[1,2]

[1] Department of Mathematics and Natural Sciences, Gulf University for Science and Technology, Mubarak Al-Abdullah, Hawally 32093, Kuwait

[2] Functional Materials Group, Gulf University for Science and Technology, Mubarak Al-Abdullah, Hawally32093, Kuwait

[3] Institut Européen des Membranes, IEM, UMR 5635, Univ Montpellier, ENSCM, Centre national de la recherche scientifique (CNRS), Place Eugène Bataillon, 34095 Montpellier, France

Tel: +965 2530 7111.

E-mail address: alameddine.b@gust.edu.kw

Contents

Synthesis of **DAC**	(i)
[1]H-NMR spectrum of **DAC**	Figure S1
[13]C-NMR spectrum of **DAC** and **ACP2,3**	Figures S2-S4
FTIR spectrum of **DAC** and **ACP2,3**	Figures S5-S7
EI-MS spectrum of **DAC**	Figure S8
XPS spectrum of **DAC** and **ACP2,3**	Figures S9-S11
TGA thermograms of **ACP1-3**	Figure S12
TGA thermograms of **ACP1-3@I_2**	Figure S13
Kinetic studies of **ACP1,2@I_2**	Figures S14, S15
N_2 adsorption and desorption isotherms for **ACP1** recorded at 77 K	Figure S16
Suggested CO_2 adsorption mechanism by **ACP3**	Figure S17
Suggested I_2 adsorption mechanism by **ACP3**	Figure S18
Comparison of CO_2 and I_2 capture capacity with different adsorbents	Tables S1, S2

(i) Synthesis of DAC

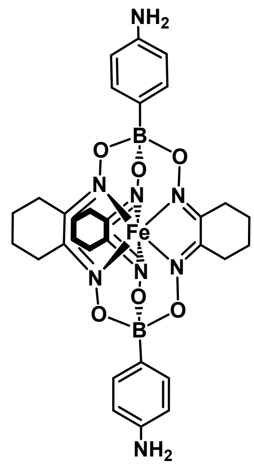

To a stirring degassed solution of 4-Aminophenylboronic acid pinacol ester (1 g, 4.56 mmol, 1 eq.) in methanol (40 mL), 1,2-cyclohexanedione dioxime (0.84 g, 5.93 mmol, 1.3 eq.) and iron(II) chloride (0.26 g, 2.05 mmol, 0.45 eq.) were added under argon and the reaction mixture was allowed to reflux for 24h. The solvent was concentrated and the red solid was precipitated from petroleum ether. The precipitate was filtered and washed thoroughly with water, petroleum ether and diethyl ether then allowed to dry under vacuum affording the desired product as a red color solid (1.38 g, 99%). ^{1}H-NMR (400 MHz, DMSO-D_6, ppm): δ 9.89 (s, 4H, -NH_2), 7.66-7.63 (d, 4H, J=12 Hz, ArH), 7.27-7.25 (d, 4H, J = 8 Hz, ArH) 2.85 (s, 12H, -CH_2), 1.76 (s, 12H, -CH_2). ^{13}C-NMR (100 MHz, DMSO-D_6, ppm): δ 168.68, 145.11, 134.15, 123.20, 109.98, 26.58 and 21.11. EI-HRMS: m/z calculated for $M^{\bullet+}$ $C_{30}H_{36}B_2FeN_8O_6$ 682.2288 found 682.3.

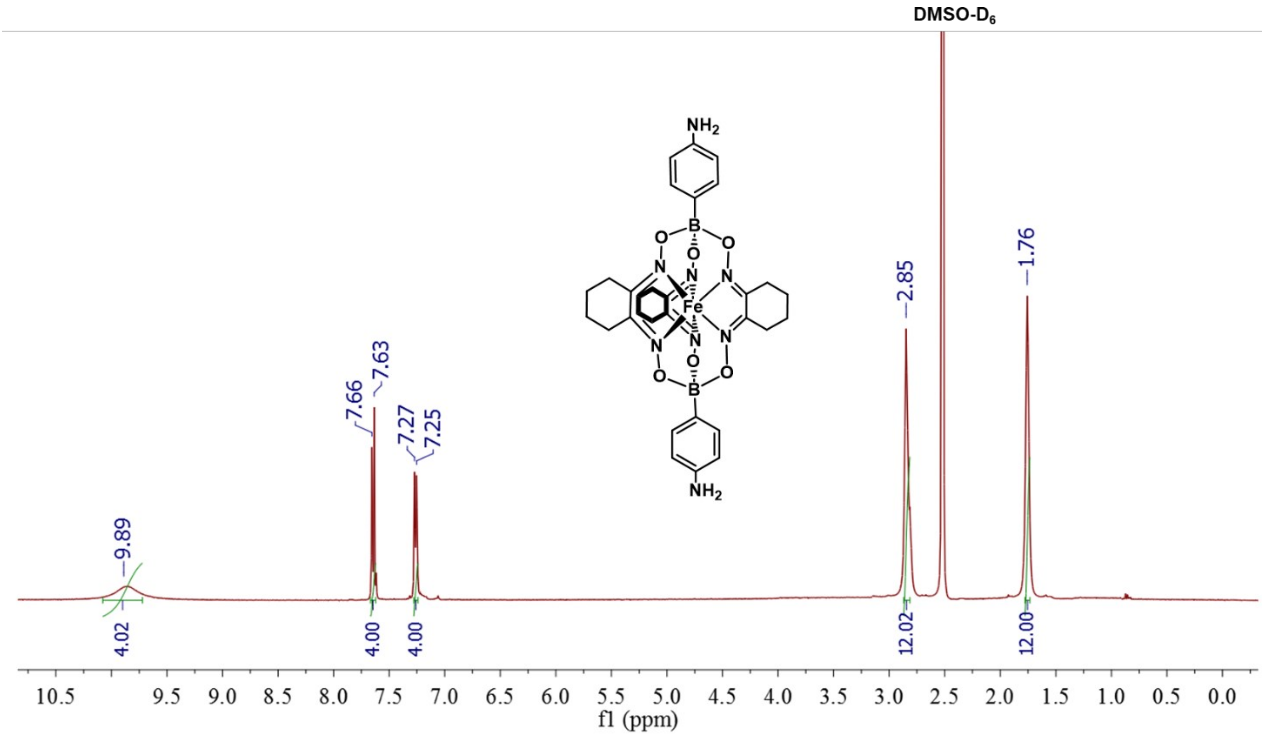

Figure S1 ^{1}H-NMR spectrum of **DAC**

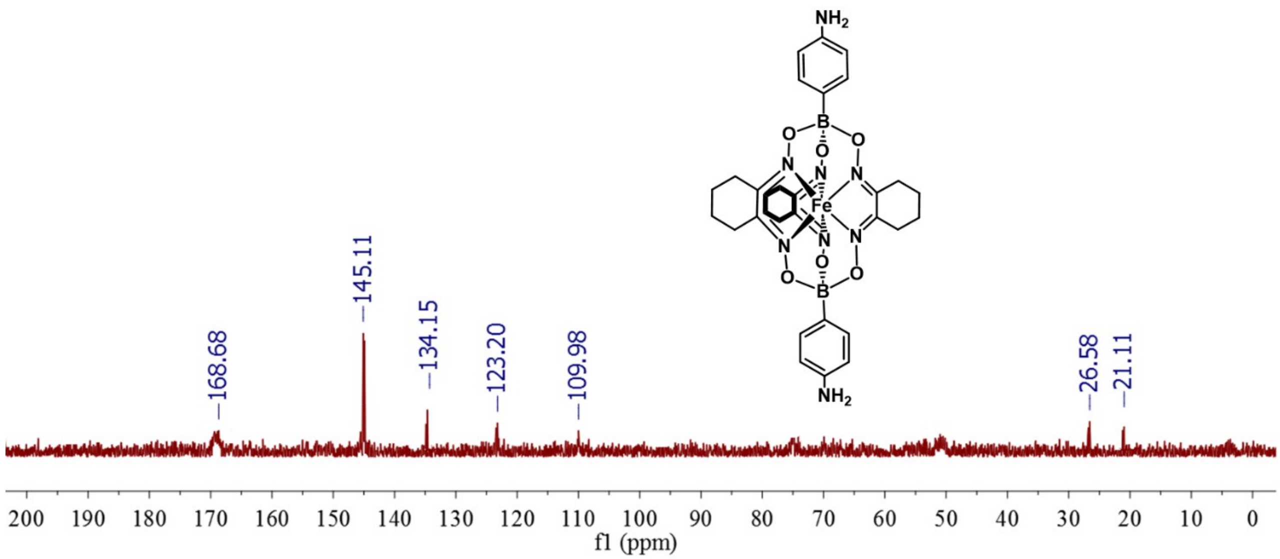

Figure S2 ^{13}C-NMR spectrum of **DAC** in DMSO-D_6

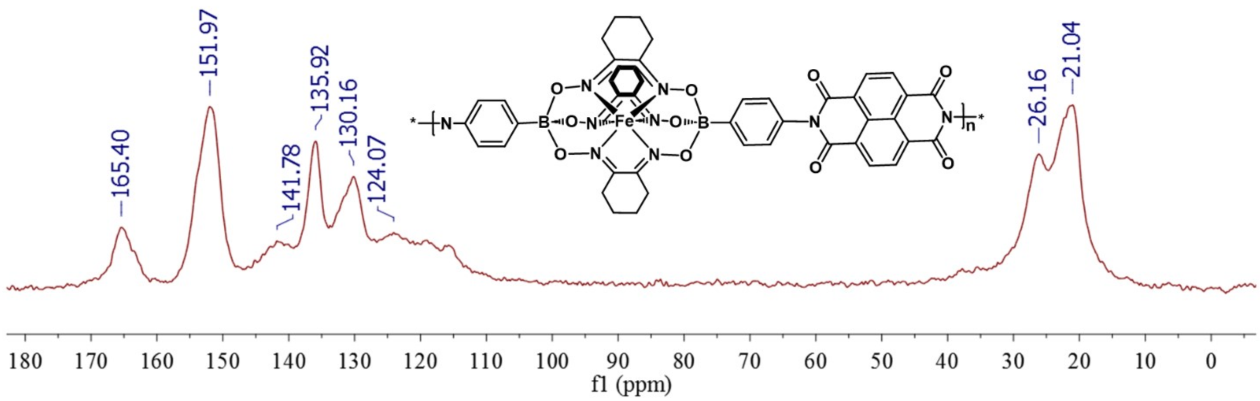

Figure S3 Solid state ^{13}C-NMR spectrum **ACP2**

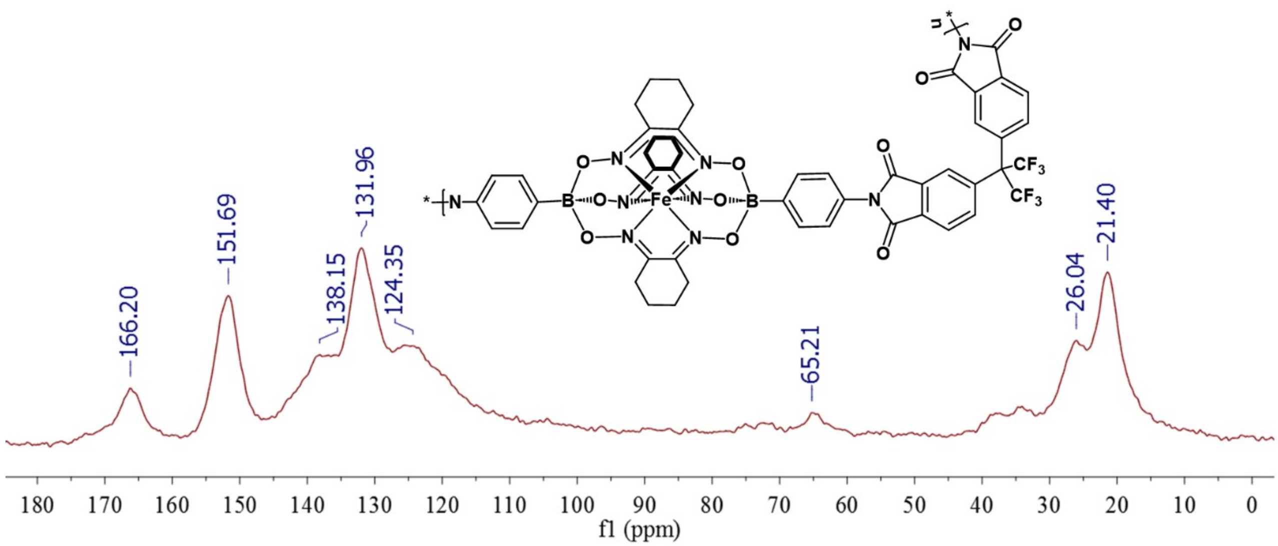

Figure S4 Solid state ^{13}C-NMR spectrum of **ACP3**

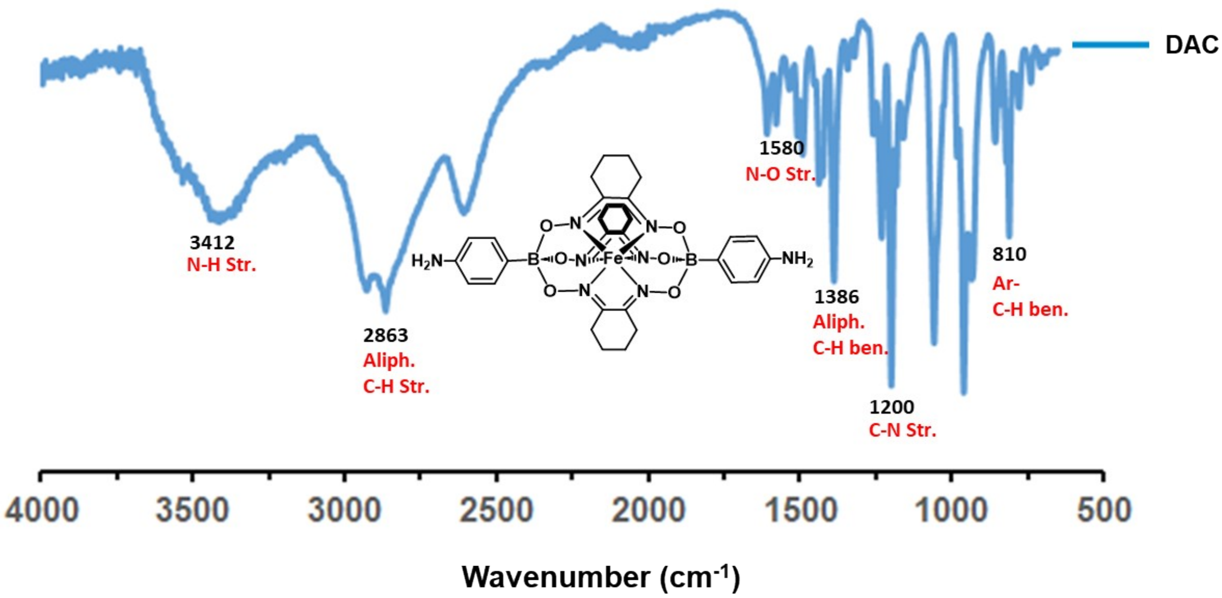

Figure S5 FTIR spectrum of **DAC**

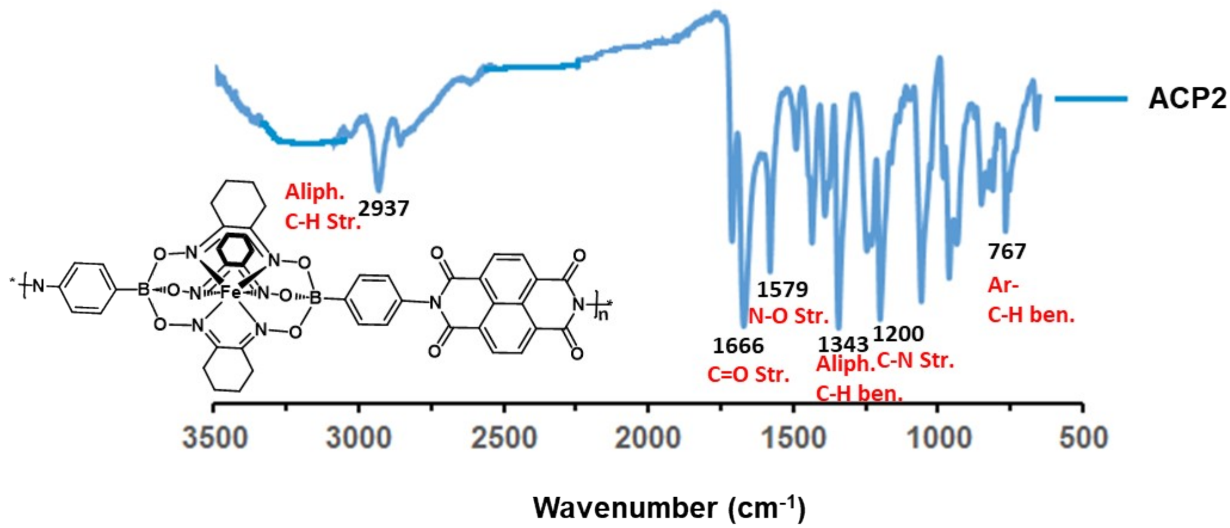

Figure S6 FTIR spectrum of **ACP2**

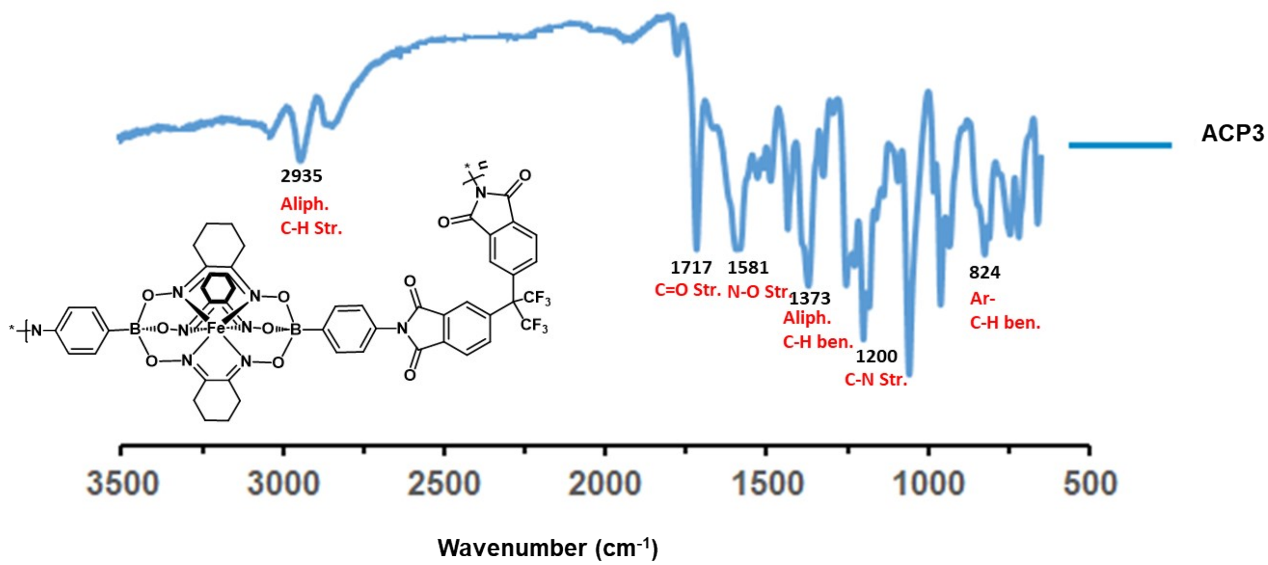

Figure S7 FTIR spectrum of **ACP3**

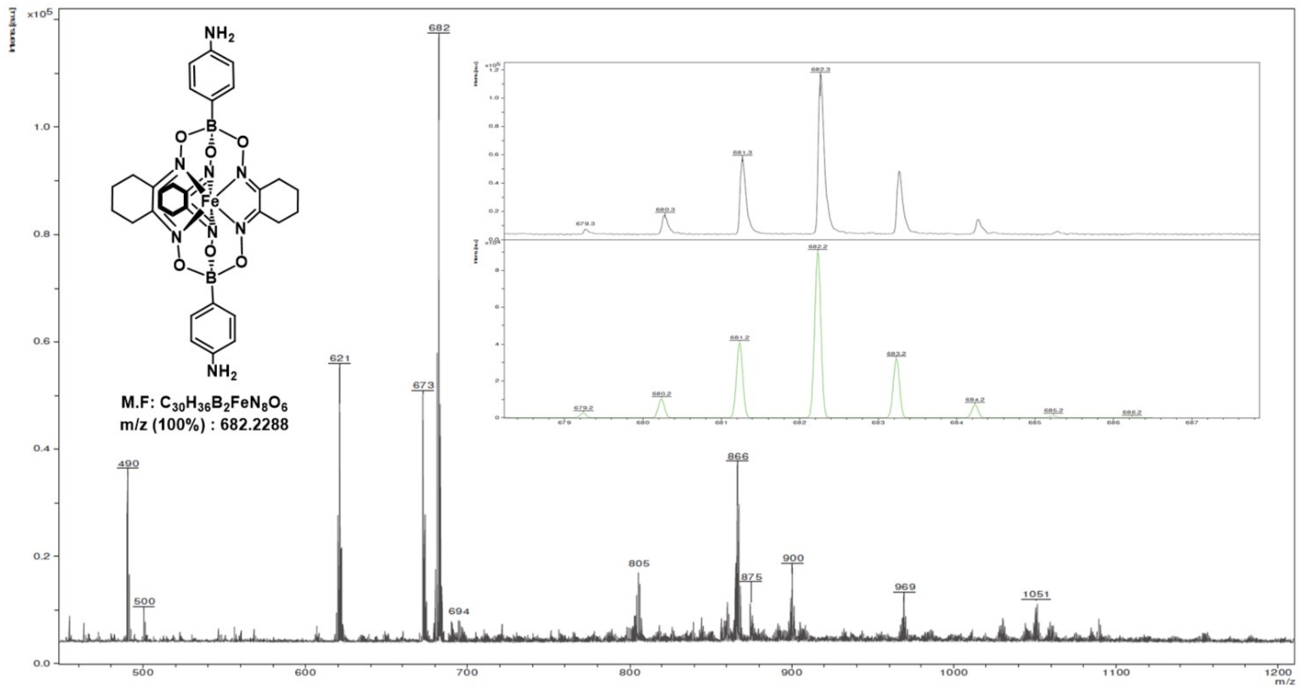

Figure S8 EI-HRMS spectrum of **DAC**

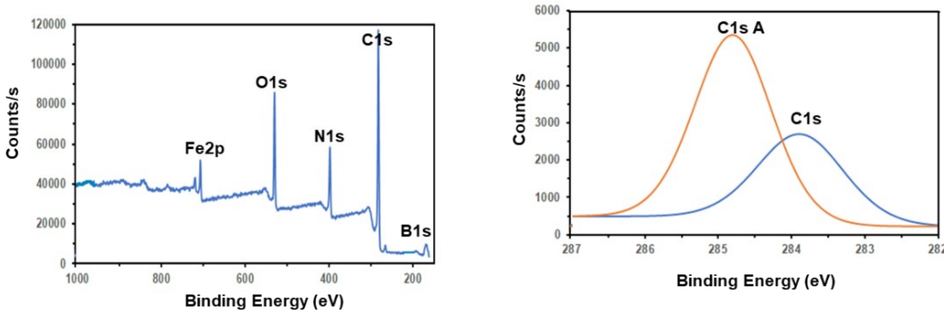

Name	Peak BE
C1s	283.89
C1s A	284.80
O1S	532.04
N1s	400.04
N1s A	401.89
Fe2p, 3/2	708.03
F22p, 1/2	721.88
B1s	190.53

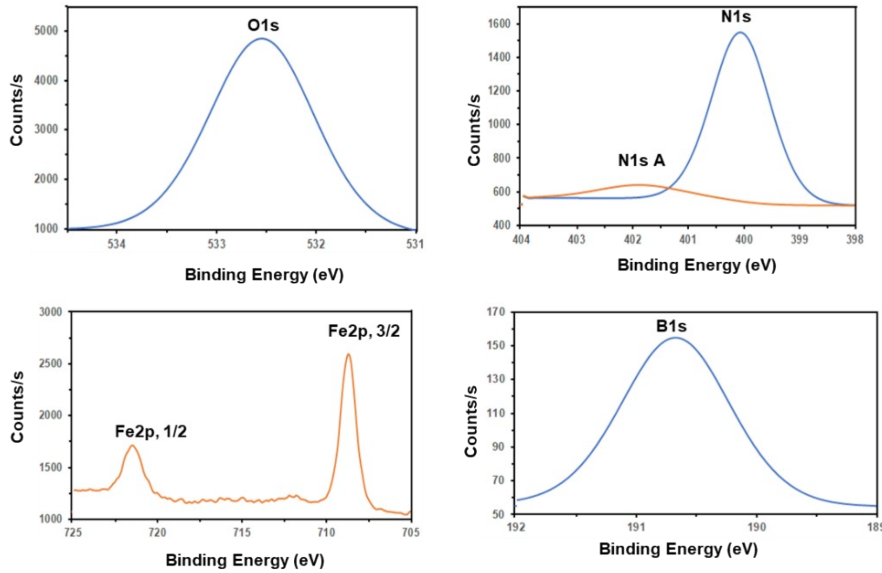

Figure S9 XPS spectrum of **DAC**

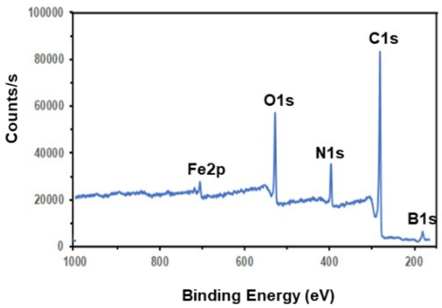

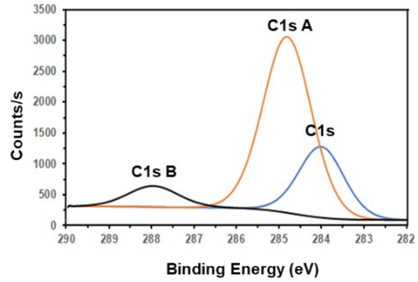

Name	Peak BE
C1s	284.00
C1s A	284.80
C1s B	287.96
O1S	530.82
O1s A	531.83
N1s	399.93
N1s A	401.47
Fe2p, 3/2	708.59
F22p, 1/2	721.88
B1s	190.48

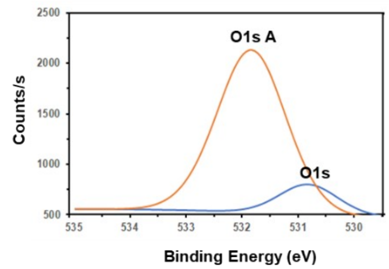

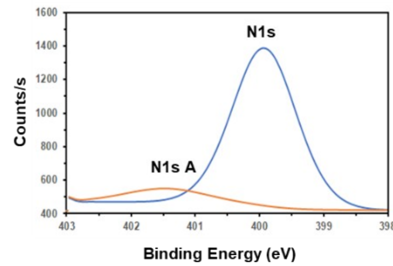

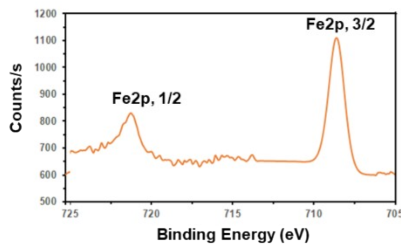

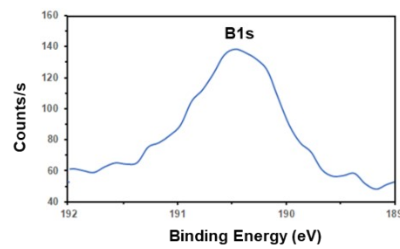

Figure S10 XPS spectrum of **ACP2**

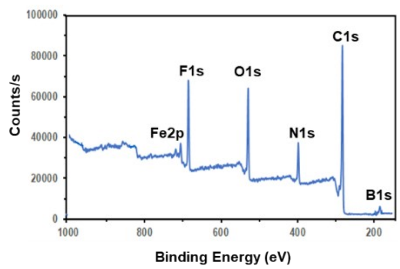

Name	Peak BE
C1s	283.99
C1s A	284.79
C1s B	287.99
C1s C	292.72
O1S	530.68
O1s A	531.89
N1s	399.97
N1s A	401.53
Fe2p, 3/2	708.36
F22p, 1/2	721.49
B1s	190.60
F1s	688.27

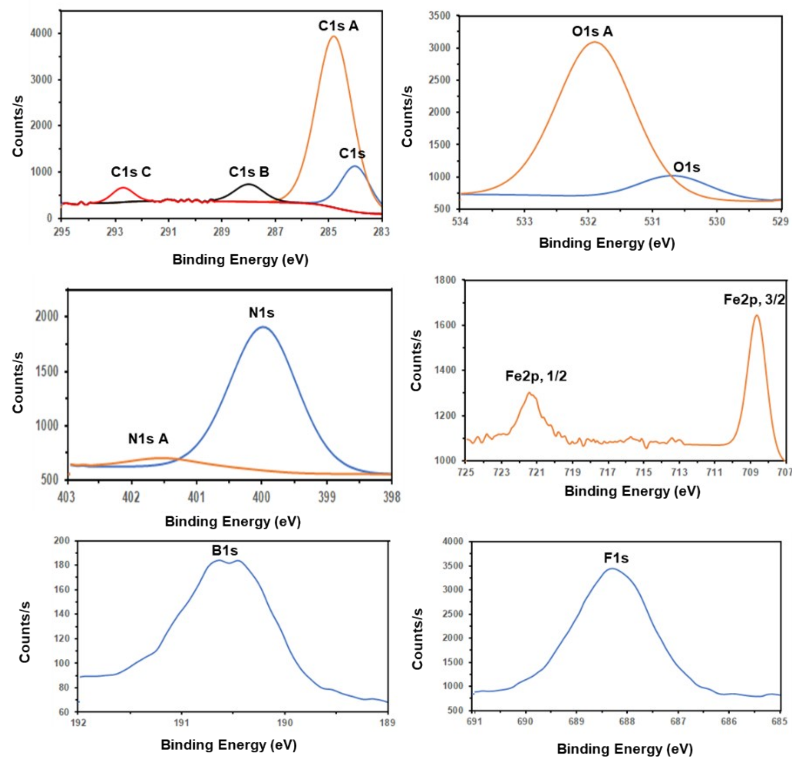

Figure S11 XPS spectrum of **ACP3**

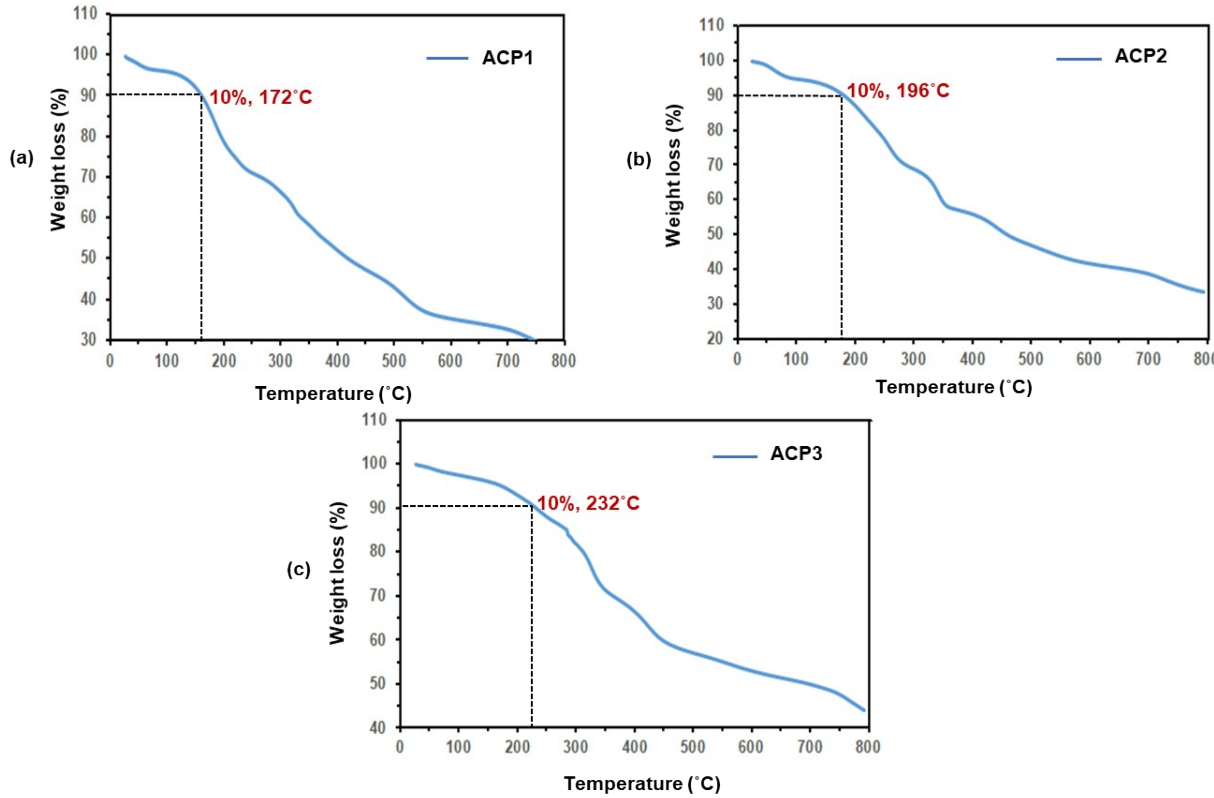

Figure S12 TGA thermograms of **(a) ACP1**, **(b) ACP2** and **(c) ACP3**, T_d represents the temperature of 10% weight loss

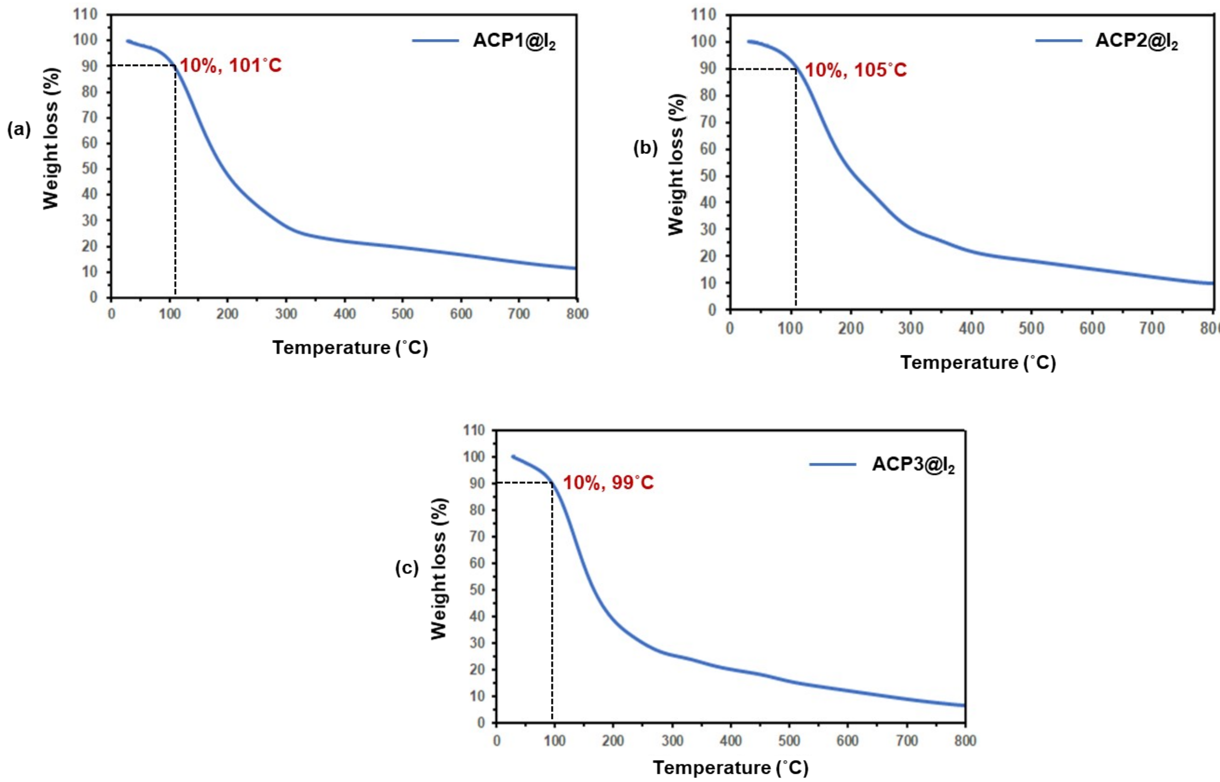

Figure S13 TGA thermograms of **(a) ACP1@I$_2$**, **(b) ACP2@I$_2$** and **(c) ACP3@I$_2$**

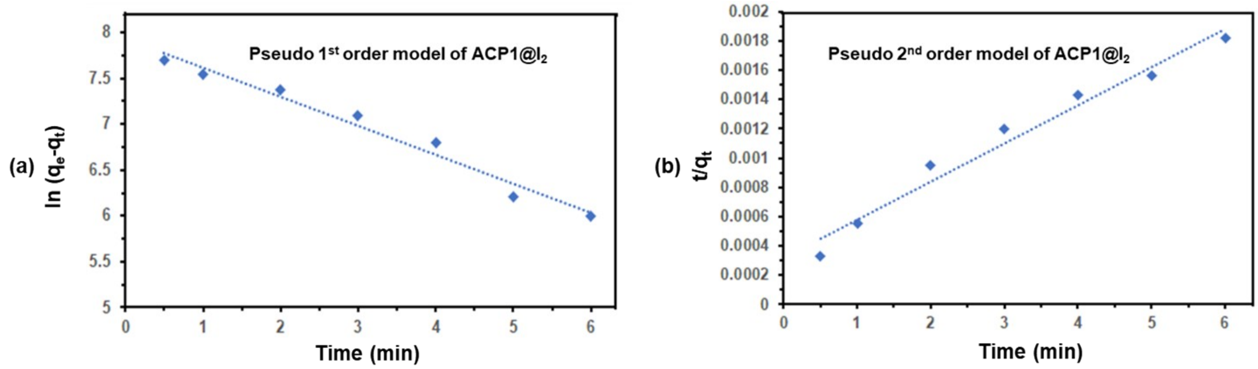

Figure S14 Pseudo-first-order **(a)** and pseudo-second-order **(b)** models of **ACP1@I_2**

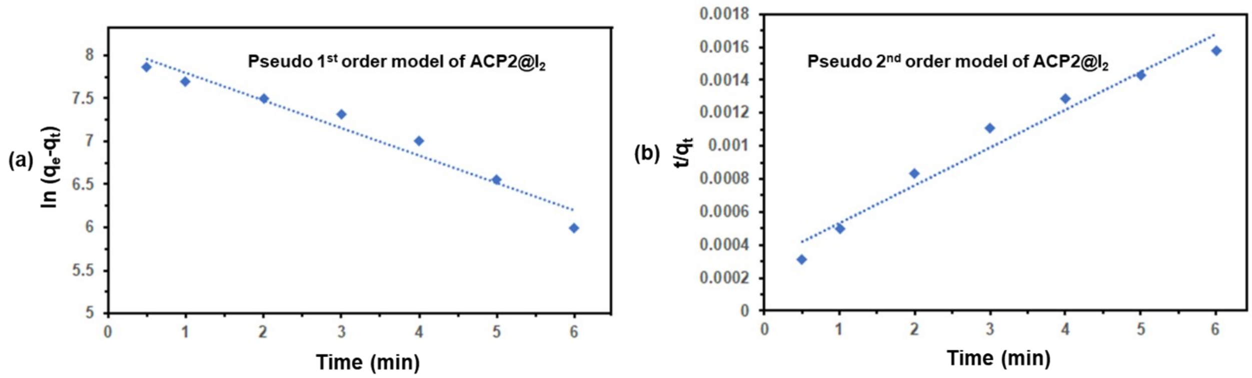

Figure S15 Pseudo-first-order **(a)** and pseudo-second-order **(b)** models of **ACP2@I_2**

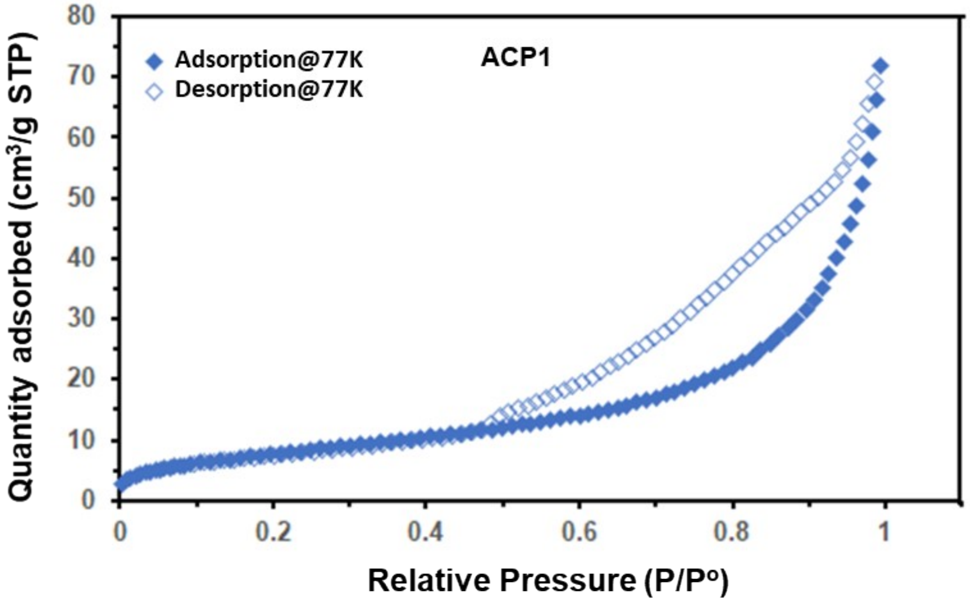

Figure S16 Nitrogen (N_2) adsorption and desorption isotherms for **ACP1** recorded at 77 K

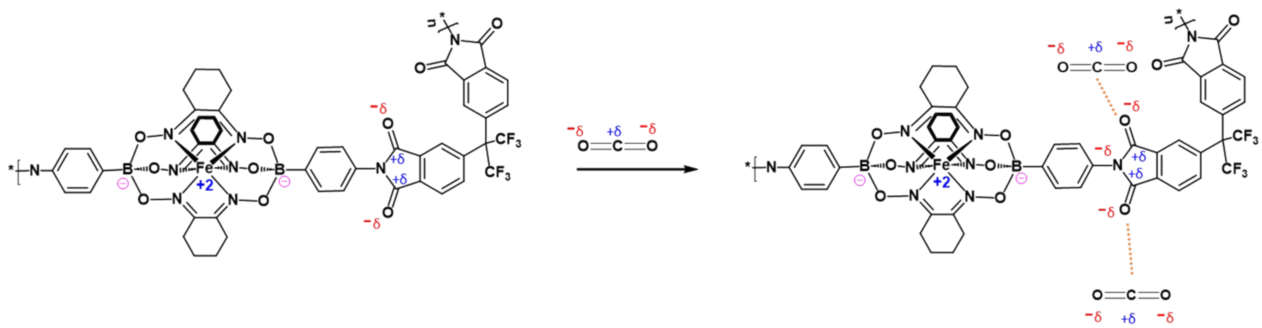

Figure S17 Suggested CO_2 adsorption mechanism by **ACP3**

Entry	Adsorbent	CO_2 (mg g^{-1})	Reference
1	Iron(II) clathrochelate based copolymers	43	This work
2	Si-MCM-41	27.3	Xu, X, 2003, Microporous and Mesoporous Materials [1]
3	Nanoporous triptycene based network polyamides (TBP3)	38	Bera, R, 2017, Polymer [2]
4	CHIT-HTC-12	4.4	Chagas, J, 2020, ACS Omega [3]

Table S1 Comparison of CO_2 capture capacity with different adsorbents

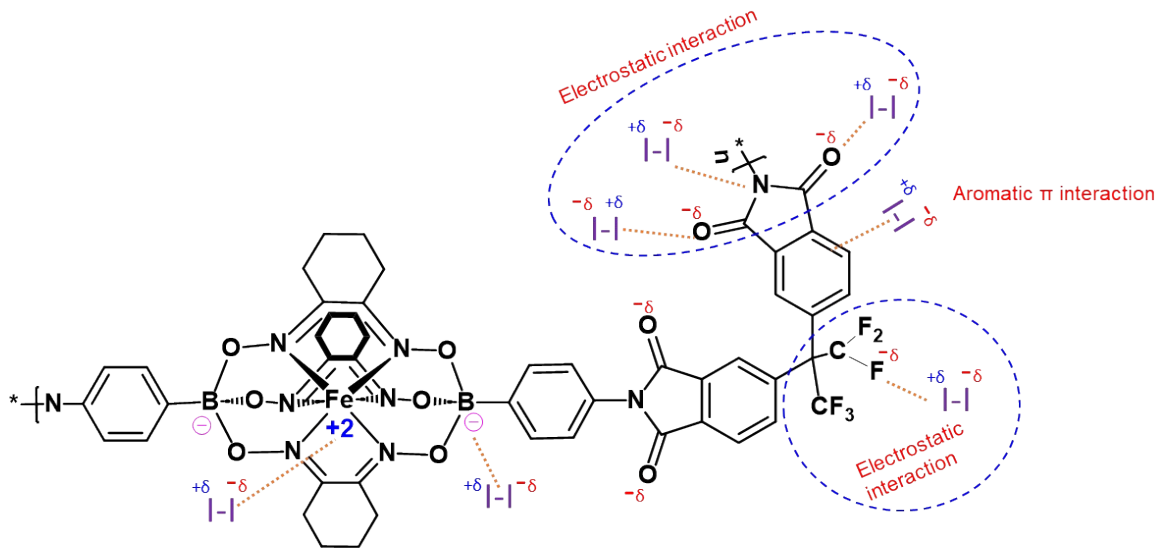

Figure S18 Suggested I_2 adsorption mechanism of by **ACP3**

Entry	Adsorbent	I_2 (wt.%)	Reference
1	Iron(II) clathrochelate based copolymers	680	This work
2	Hydroxyl-functionalized hyper-crosslinked polymers	673	Wang, J , 2024, iScience [4]
3	Conjugated Microporous Polymers Based on Octet and Tetratopic Linkers	367	Luo, S, 2023, ACS Applied Materials & Interfaces [5]
4	POP-T	394	Tian, P, 2022, Molecules [6]
5	Metal–Organic Framework Nanosheets	351	Yu, C.-X, 2022, Inorganic Chemistry [7]
6	Triazole-linked porous cage polymers	402	Begar, F, 2024, ACS Applied Polymer Materials [8]
7	Aniline-based hypercrosslinked polymers	596	Liu, B, 2023, International Journal of Molecular Sciences[9]
8	Triptycene based covalent organic polymers	486	Hassan, A, 2022, Chemical Engineering Journal [10]
9	TAPB-QOT COP	464	Yildirim, O, 2023, ACS Appl Mater Interfaces [11]
10	Triazine-based covalent organic polymers (POPs-1)	441	Xiong, S, 2023, Journal of Materials Research and Technology [12]

Table S2 Comparison of I_2 capture capacity with different adsorbents

References

(1) Xu, X.; Song, C.; Andrésen, J. M.; Miller, B. G.; Scaroni, A. W. Preparation and Characterization of Novel CO_2 “Molecular Basket” Adsorbents Based on Polymer-Modified Mesoporous Molecular Sieve MCM-41. Microporous and Mesoporous Materials 2003, 62 (1), 29-45. DOI: 10.1016/S1387-1811(03)00388-3.

(2) Bera, R.; Mondal, S.; Das, N. Nanoporous Triptycene Based Network Polyamides (TBPs) for Selective CO_2 Uptake. Polymer 2017, 111, 275-284. DOI: 10.1016/j.polymer.2017.01.056.

(3) Chagas, J. A. O.; Crispim, G. O.; Pinto, B. P.; San Gil, R. A. S.; Mota, C. J. A. Synthesis, Characterization, and CO_2 Uptake of Adsorbents Prepared by Hydrothermal Carbonization of Chitosan. ACS Omega 2020, 5 (45), 29520-29529. DOI: 10.1021/acsomega.0c04470.

(4) Wang, J.; Wu, T.; Wang, X.; Chen, J.; Fan, M.; Shi, Z.; Liu, J.; Xu, L.; Zang, Y. Construction of Hydroxyl-Functionalized Hyper-Crosslinked Networks from Polyimide for Highly Efficient Iodine Adsorption. iScience 2024, 27 (2), 108993. DOI: 10.1016/j.isci.2024.108993.

(5) Luo, S.; Yan, Q.; Wang, S.; Hu, H.; Xiao, S.; Su, X.; Xu, H.; Gao, Y. Conjugated Microporous Polymers Based on Octet and Tetratopic Linkers for Efficient Iodine Capture. ACS Applied Materials & Interfaces 2023, 15 (39), 46408-46416. DOI: 10.1021/acsami.3c10786.

(6) Tian, P.; Ai, Z.; Hu, H.; Wang, M.; Li, Y.; Gao, X.; Qian, J.; Su, X.; Xiao, S.; Xu, H.; et al. Synthesis of Electron-Rich Porous Organic Polymers via Schiff-Base Chemistry for Efficient Iodine Capture. Molecules, 2022, 27(16), 5161. DOI: 10.3390/molecules27165161

(7) Yu, C.-X.; Li, X.-J.; Zong, J.-S.; You, D.-J.; Liang, A.-P.; Zhou, Y.-L.; Li, X.-Q.; Liu, L.-L. Fabrication of Protonated Two-Dimensional Metal–Organic Framework Nanosheets for Highly

Efficient Iodine Capture from Water. Inorganic Chemistry 2022, 61 (35), 13883-13892. DOI: 10.1021/acs.inorgchem.2c01886.

(8) Begar, F.; Erdogmus, M.; Gecalp, Y.; Canakci, U. C.; Buyukcakir, O. Synthesis of Triazole-Linked Porous Cage Polymers: Modulating Cage Size for Tailored Iodine Adsorption. ACS Applied Polymer Materials 2024. DOI: 10.1021/acsapm.4c00560.

(9) Liu, B.; Mao, C.; Zhou, Z.; Wang, Q.; Zhou, X.; Liao, Z.; Deng, R.; Liu, D.; Beiyuan, J.; Lv, D.; et al. Two Facile Aniline-Based Hypercrosslinked Polymer Adsorbents for Highly Efficient Iodine Capture and Removal. International Journal of Molecular Sciences, 2023, 24 (1), 370 DOI: 10.3390/ijms24010370.

(10) Hassan, A.; Alam, A.; Ansari, M.; Das, N. Hydroxy Functionalized Triptycene Based Covalent Organic Polymers for Ultra-high Radioactive Iodine Uptake. Chemical Engineering Journal 2022, 427, 130950. DOI: 10.1016/j.cej.2021.130950

(11) Yildirim, O.; Tsaturyan, A.; Damin, A.; Nejrotti, S.; Crocellà, V.; Gallo, A.; Chierotti, M. R.; Bonomo, M.; Barolo, C. Quinoid-Thiophene-Based Covalent Organic Polymers for High Iodine Uptake: When Rational Chemical Design Counterbalances the Low Surface Area and Pore Volume. ACS Appl Mater Interfaces 2023, 15 (12), 15819-15831. DOI: 10.1021/acsami.2c20853.

(12) Xiong, S.; Huang, H.; Tang, T.; Cao, X.; Zhao, H.; Li, G.; Liu, H.; Zhang, W.; Liu, Q. Creating high-affinity binding sites for efficient CO_2 and iodine vapor uptake through direct synthesis of novel triazine-based covalent organic polymers. Journal of Materials Research and Technology 2023, 27, 5629-5638. DOI: 10.1016/j.jmrt.2023.10.309